

Resonant soft x-ray emission as a bulk probe of correlated electron behavior in metallic $\text{Sr}_x\text{Ca}_{1-x}\text{VO}_3$

J. Laverock,¹ B. Chen,¹ K. E. Smith,¹ R. P. Singh*,² G. Balakrishnan,²
M. Gu,³ J. W. Lu,⁴ S. A. Wolf,^{3,4} R. M. Qiao,⁵ W. Yang,⁵ and J. Adell⁶

¹*Department of Physics, Boston University, 590 Commonwealth Avenue, Boston, Massachusetts, MA 02215, USA*

²*Department of Physics, University of Warwick, Coventry, CV4 7AL, United Kingdom*

³*Department of Physics, University of Virginia, Charlottesville, VA 22904, USA*

⁴*Department of Materials Science and Engineering,
University of Virginia, Charlottesville, VA 22904, USA*

⁵*Advanced Light Source, Lawrence Berkeley National Laboratory, Berkeley, California, CA 94720, USA*

⁶*MAX-lab, Lund University, SE-221 00 Lund, Sweden*

The evolution of electron correlation in $\text{Sr}_x\text{Ca}_{1-x}\text{VO}_3$ has been studied using a combination of bulk-sensitive resonant soft x-ray emission spectroscopy (RXES), surface-sensitive photoemission spectroscopy (PES), and *ab initio* band structure calculations. We show that the effect of electron correlation is enhanced at the surface. Strong incoherent Hubbard subbands are found to lie $\sim 20\%$ closer in energy to the coherent quasiparticle features in surface-sensitive PES measurements compared with those from bulk-sensitive RXES, and a $\sim 10\%$ narrowing of the overall bandwidth at the surface is also observed.

Understanding correlated electron behavior remains one of the most important problems in condensed matter physics. In correlated electron systems, the interaction between electrons is of the order of, or larger than, the electron kinetic energy, and the concept of a well-defined quasiparticle is restricted to a narrow region of energies near the Fermi level, beyond which our strict understanding of a quasiparticle with a defined dispersion relation, easily accessible through band theory, breaks down. Rather, the competition between itinerant delocalized behavior and strongly-correlated localized behavior leads to the transfer of spectral weight away from the quasiparticle peak (QP) and into incoherent Hubbard subbands.[1]

As a probe of correlated electron behavior, angle-resolved photoemission spectroscopy (ARPES) is uniquely placed: It is capable of measuring the many-body electron dispersion relation, $E(\mathbf{k})$, with high precision, including the Fermi surface (FS) and modifications to $E(\mathbf{k})$ that are due to the coupling of the electrons to collective excitations.[2] However, owing to the short mean free path of the photoelectrons, ARPES is intrinsically a surface sensitive probe, particularly of three-dimensional (3D) systems, and is usually limited to within 15 Å of the surface (although efforts to enhance the bulk sensitivity, such as laser-ARPES can yield information to over 100 Å).[3] On the other hand, resonant soft x-ray emission spectroscopy (RXES), being a photon-in-photon-out technique, is truly a probe of the *bulk* electronic structure, with a typical sampling depth of ~ 100 nm.[4]

Here, we demonstrate that RXES is a sensitive probe of correlated electron behavior, capable of yielding com-

plementary information to ARPES from a truly *bulk* perspective. Specifically, we show that electron-electron correlation in $\text{Sr}_x\text{Ca}_{1-x}\text{VO}_3$ is enhanced near the sample surface. We accomplish this through comparison of RXES measurements with photoemission spectroscopy (PES) measurements on the same $\text{Sr}_x\text{Ca}_{1-x}\text{VO}_3$ single crystal samples, as well as on CaVO_3 thin film samples. Our RXES results are in much closer agreement with dynamical mean-field theory (DMFT) calculations than the PES results; in these calculations the value of the Hubbard U parameter has been determined from first principles.[5] Our RXES data explain the discrepancy between numerous published ARPES measurements of $\text{Sr}_x\text{Ca}_{1-x}\text{VO}_3$,[6–10] and between ARPES and DMFT calculations.[5, 11, 12] Moreover, these results illustrate the powerful application that RXES can have in addressing correlated electron behavior, particularly when comparisons can be directly made with (AR)PES measurements, and they shed light on the different scattering mechanisms of the two techniques.

The $\text{Sr}_x\text{Ca}_{1-x}\text{VO}_3$ ($0 \leq x \leq 1$) family of oxides are prototypical strongly-correlated materials, exhibiting both strong Hubbard subbands as well as appreciable quasiparticle peaks.[5, 9] These materials have been well studied with ARPES, but the results have yielded conflicting pictures of the role of electron correlations. Measurements aimed at extracting “bulk” ARPES spectra have been performed at both high[6] and low[7] incident photon energies (i.e. away from the minimum in the photoelectron mean free path). These studies reported either spectra that were independent of x ,[6] or a weak suppression of the QP in CaVO_3 . [7] More recent ARPES measurements, in which FSs and band dispersions were clearly observed in both end-members, suggest both a narrowing of the bandwidth and a suppression of the QP in CaVO_3 compared with SrVO_3 , [9] consistent with expectations that CaVO_3 experiences stronger electron correlations. The role of the surface in ARPES mea-

*Present address: Department of Physics, IISER Bhopal, MP-462023, India

measurements has been questioned throughout,[12, 13] and confirmation from a truly bulk probe is clearly desirable.

In the transition-metal L -edge RXES process, a $2p$ core electron is excited into the conduction band in analogy with the x-ray absorption process. The excited state subsequently decays to fill the core hole, in which the energy and, in principle momentum, of the emitted x-ray is measured.[14] The core hole can decay via several routes: (i) elastic scattering, in which the excited electron returns to the original core level without transferring energy to the system, (ii) inelastic scattering, in which energy is transferred to the system during the intermediate state, in the form of either localized or delocalized excitations (i.e. Raman-type resonant inelastic x-ray scattering, RIXS), and (iii) fluorescent-like core hole decay, in which an electron from an occupied valence band state makes the transition to the core hole. Both (i) and (ii) yield features whose energy depends on the incident photon, whereas the energy of (iii) is independent of the excitation energy. In this work, we will focus on (iii), i.e. the normal x-ray emission-like part of the spectrum.

Large high quality single crystals of CaVO_3 (CVO) and $\text{Sr}_{0.5}\text{Ca}_{0.5}\text{VO}_3$ (SCVO) were grown by the floating zone technique in a four mirror optical furnace, employing growth rates of 7 to 10 mm/h in an atmosphere of 1 bar of Ar + 3% H_2 gas.[15] Samples for the RXES measurements were obtained by cleaving the as grown crystals *ex-situ*, and were immediately loaded into the ultra-high vacuum chamber. RXES and x-ray absorption spectroscopy (XAS) measurements were performed at beamline 8.0.1 of the Advanced Light Source, Lawrence Berkeley National Laboratory. The resolution of the emission spectrometer was 0.35 eV at full-width half maximum (FWHM). XAS measurements, recorded in both total electron yield (TEY, sampling depth ~ 10 nm) and total fluorescent yield (TFY, sampling depth ~ 100 nm) were recorded with an energy resolution of 0.2 eV. For ARPES measurements, clean well-ordered surfaces were prepared by cleaving *in-situ* in ultra high vacuum, and were oriented with reference to low-energy electron diffraction patterns. (AR)PES measurements were performed at beamline I4 at the MAXlab synchrotron radiation facility (Lund, Sweden). The incident photon energy was 80 eV and the total instrument electron energy resolution was 25 meV. Measurements of the FS and band dispersion of both samples (not presented here) are in good agreement with previously published work.[9, 10] The sampling depth of the RXES measurements is estimated to be ~ 100 nm, which can be compared with the photoelectron mean free path of ~ 0.5 nm for our ARPES measurements (at 80 eV). Correspondingly, previous “bulk-sensitive” ARPES measurements recorded at a photon energy of 900 eV reach less than 2 nm into the sample (in that work, the surface depth was estimated to be 0.5 – 1 nm).[6] Thin (46 nm) CVO films were grown on $\text{SrTiO}_3(001)$ substrates using a pulsed electron-beam deposition technique,[16] and were capped with a 2.5 nm SrTiO_3 layer to protect the surface of

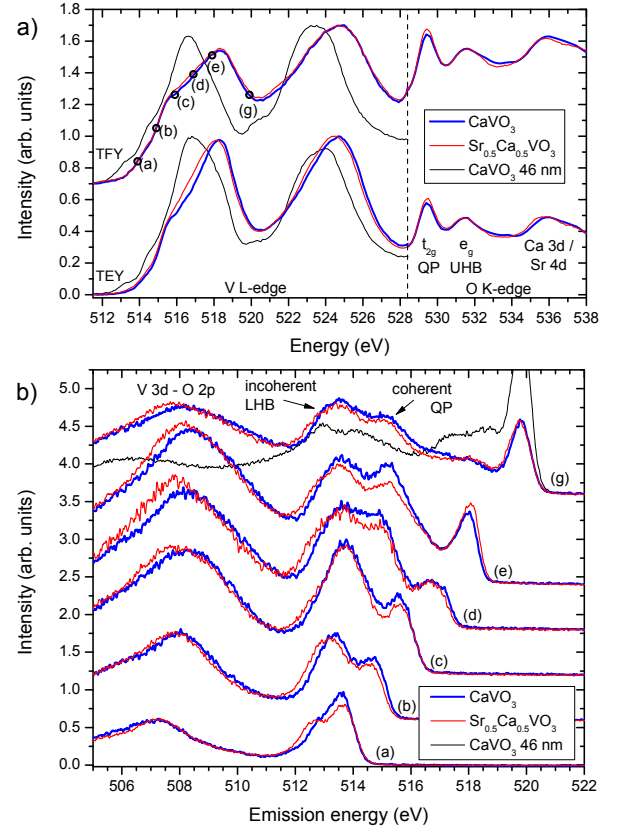


FIG. 1: (Color online) Bulk (a) XAS and (b) RXES measurements of CVO and SCVO. The spectra of a 46 nm thin film of CVO[16] are also shown for comparison. The excitation energies used in the RXES measurements of (b) are shown by the circles in (a). The vertical line in (a) indicates separate V L -edge (left) and O K -edge (right) measurements, which have been separately scaled for clarity.

CVO, precluding measurements at the O K -edge and ARPES. *Ab initio* calculations of the electronic structure of cubic perovskite SrVO_3 and orthorhombic (distorted perovskite)[17] CaVO_3 were performed with the all electron full potential linearized augmented plane wave ELK code[18] within the local density approximation (LDA). Convergence was achieved on 84 k-points in the irreducible Brillouin zone (IBZ) of cubic SrVO_3 and on 343 k-points in the orthorhombic IBZ of CaVO_3 .

V L -edge and O K -edge XAS and RXES spectra are shown for CVO and SCVO in Fig. 1. XAS spectra at the V L -edge are very similar for the two compounds (shown in both TEY and TFY modes in Fig. 1a), and are in close agreement with previous measurements.[19] These spectra are not well described by atomic multiplet calculations owing to the itinerant behavior of the metallic V d electrons.[19] At the O K -edge, which is sensitive to the unoccupied conduction band partial density of states (PDOS), three features dominate the spectra and are related to excitations into V t_{2g} and e_g states, as well as excitations into the Ca/Sr d states at higher energies. DMFT calculations of the V t_{2g} states predict that

the upper Hubbard band (UHB) overlaps with the e_g feature, whereas the t_{2g} XAS feature encompasses the coherent QP peak.[5] An alternative description, based on extended cluster model calculations, also suggests that the t_{2g} feature involves excitations into the coherent metallic states.[20] In Fig. 1a, the ratio of the t_{2g} to e_g intensities is found to be slightly higher in SCVO than in CVO, reflecting the larger QP weight that accompanies the “weaker” correlations in this compound, in agreement with DMFT[5] as well as ARPES measurements of the occupied states.[9]

RXES measurements across the V L_3 -edge are shown in Fig. 1b. At low energies, the peak centered at 508 eV is due to V $3d - O 2p$ hybridization,[21] whereas the V $3d$ states appear in the range 512 – 516 eV. The constant emission energy of this feature establishes its origin as fluorescent-like decay of the core hole rather than Raman-type loss features, which are weak for metallic systems. The dispersive peak is predominantly due to elastically scattered x-rays, and is centered at the incident photon energy of each spectrum. As the incident photon energy is tuned through the V L_3 -edge, emission from the available V $3d$ states is resonantly enhanced. For spectrum (f), which is recorded above the V L_3 -edge absorption feature, the resonance effects on the fluorescent part of the spectrum are weak, and we interpret this spectrum as most closely representing the occupied V $3d$ PDOS. Moreover, at this energy, low-energy loss features (which are typically $\lesssim 4$ eV)[21] are well separated from the fluorescent part of the spectrum.

In spectra (d-f), the V $3d$ fluorescence is split into a double-peaked structure, which can be associated with the incoherent lower Hubbard band (LHB) and coherent QP electron states, as suggested by LDA+DMFT calculations[5] and observed in ARPES measurements.[9] Whilst the energy of the coherent feature is similar for both compounds, the incoherent feature of the Sr-doped compound is spread to lower energies, and the peak is centered 0.1 – 0.2 eV lower than CVO. Quantitatively, we find that the separation between coherent and incoherent features is 1.4 and 1.6 eV for CVO and SCVO respectively. Note that this is the separation between the centers of the two RXES features, and does not necessarily reflect the fundamental energy separation between LHB and QP states. Nevertheless, the evolution in this separation can be associated with the evolution in electron correlations in going from SrVO₃ to CaVO₃, usually identified as a consequence of the narrowing of the bandwidth. The bandwidth is difficult to experimentally assess from these RXES spectra, owing to the broad nature of the features. However, by analyzing the first derivative of the spectra, it is possible to estimate the total bandwidth of the incoherent + coherent V $3d$ states, which we find to be 3.0 and 3.2 eV for CVO and SCVO respectively (i.e. an increase of $\sim 10\%$, consistent with our band structure calculations). In our surface-sensitive ARPES spectra, the bottom of the t_{2g} band (at Γ) was observed at 0.44 eV and 0.49 eV for CVO and SCVO respectively,

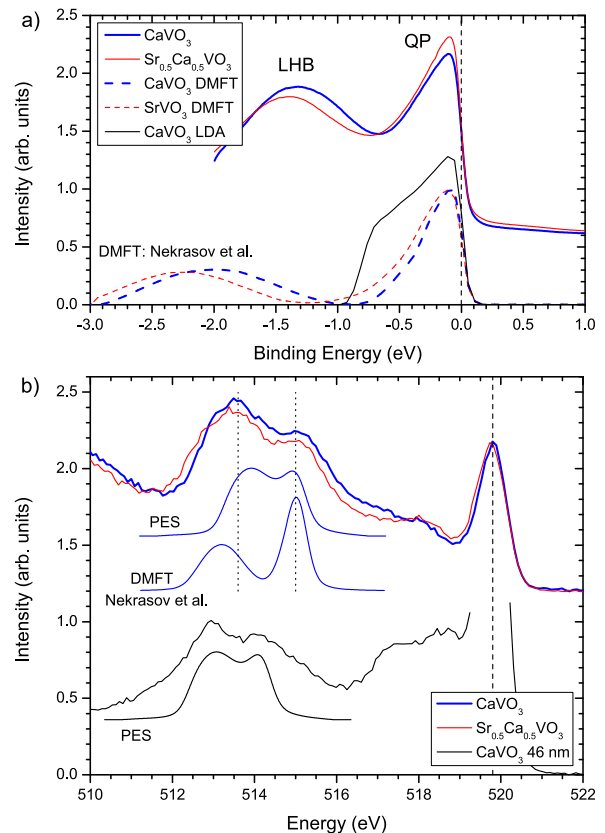


FIG. 2: (Color online) Comparison of PES and RXES spectra. (a) PES spectra of CVO and SCVO compared with the LDA DOS of CaVO₃ and DMFT calculations of CaVO₃ and SrVO₃ (reproduced from Ref. [5]). (b) PES spectra compared with the RXES spectra at excitation energy (f). The PES and DMFT spectra have been broadened to approximate the RXES measurement (see text), and the RXES spectra are shown rebinned to double the statistical precision.

in agreement with these bulk estimations.

Additional support for this interpretation is provided through comparison with thin film (46 nm) CaVO₃. Spectra of this sample at the V L -edge are shown alongside the single crystal data in Fig. 1. In the XAS, the thin film spectra are markedly different from those of the bulk single crystals, and more closely resemble the results of atomic multiplet calculations of the V d^1 ion[19] and other V⁴⁺ oxides (e.g. VO₂)[21], indicating the suppression of itinerant electron behavior and the corresponding relevance of the localized electron picture. The strong elastic peak and relative enhancement of Raman-type loss features in the RXES (Fig. 1b) are also indicative of more localized electron behavior. Moreover, the separation between the incoherent and coherent V $3d$ features is much closer than for the single crystal CaVO₃ at 1.1 eV, $\sim 20\%$ lower than bulk CaVO₃. Correspondingly, the overall (coherent + incoherent) bandwidth of thin film CaVO₃ is reduced by $\sim 10\%$ to 2.7 eV. Together, these results indicate that the electron correlations in thin film CaVO₃ are substantially exaggerated compared with the

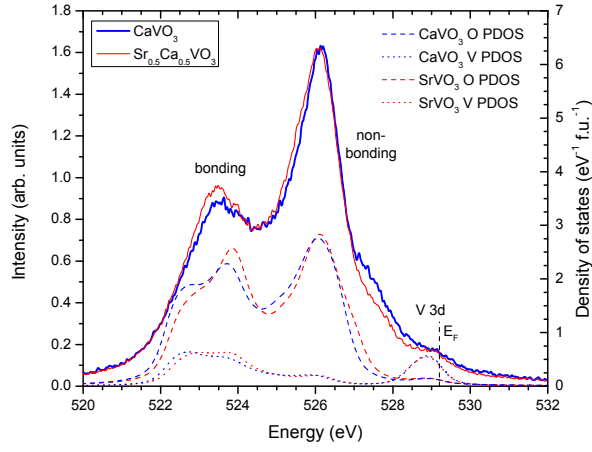


FIG. 3: (Color online) O K -edge XES spectra of CVO and SCVO. The corresponding O and V PDOS from the LDA are shown for comparison after convolution with a Lorentzian of 0.22 eV HWHM and a Gaussian of 0.35 eV FWHM to account for lifetime and instrument broadening respectively. The E_F corresponds to that of the LDA calculations.

bulk material. Indeed, for thicknesses of $\lesssim 4$ nm, CaVO_3 has been found to exhibit a metal-insulator transition at ~ 100 K.[16] RXES measurements of 4 nm thick CaVO_3 (not presented here owing to the weak count rate of these very thin samples) showed similar spectral features to 46 nm samples.

In Fig. 2, we compare the RXES spectra at excitation energy (f) with angle-integrated PES measurements, recorded with a photon energy of 80 eV. These PES measurements (Fig. 2a) exhibit the typical double-peaked structure of the LHB and QP that have previously been reported for CaVO_3 and SrVO_3 ,[7, 9] including the transfer of spectral weight from the QP to the LHB, and the shift to lower binding energies of the LHB in CaVO_3 . Indeed, such an evolution is predicted by DMFT (the DMFT of Nekrasov *et al.*[5] are reproduced, multiplied by the Fermi function, for comparison in Fig. 2), and stems from the increased importance of electron-electron correlations (often characterised as U/W) compared with the narrower bandwidth, W , of CaVO_3 . In Fig. 2b, the V 3d PES spectrum of CaVO_3 is shown after convolution with a Lorentzian of 0.1 eV HWHM (half-width half maximum) and a Gaussian of 0.35 eV FWHM to approximate the finite lifetime and instrument broadening respectively, and shifted in energy to align the high energy QP features. Whilst the double-peaked structure of the broadened PES spectrum is reproduced by the bulk-sensitive RXES measurement, the energy separation between the LHB and QP is larger in the bulk. On the other hand, a similar broadening of the DMFT CaVO_3 results leads to an overestimation of this separation. These results indicate that the LHB appears closer to the QP in surface-sensitive measurements, whereas the bulk-sensitive RXES measurements are in better agreement with DMFT predictions based on a first-principles

calculation of U . [5] We note that in an early PES study surface disorder was found to shift the LHB further from E_F , [22] suggesting the differences we observe are intrinsically linked to the surface. Indeed, such an enhancement in the effects of electron correlation at the surface is predicted by DMFT calculations of the SrO-terminated layer of SrVO_3 , in which the LHB was found to be 40% closer to the QP than calculations of the bulk.[12] We note that this effect is already present in calculations of the idealized (unrelaxed) surface,[12] indicating the enhancement in correlated behavior is a fundamental property of the surface. In the lower part of Fig. 2b, RXES spectrum (f) is shown of the CaVO_3 46 nm thin film, alongside the same (broadened) PES spectrum (and shifted to approximately align the QP). As can be seen, the PES and RXES features are in much better agreement for this sample, in which the surface contribution to the RXES measurement dominates over the bulk. The longer low-energy tail of this spectrum (extending below 512 eV) may represent a small bulk-like volume of the thin-film.

Finally, in Fig. 3, the O K -edge normal XES spectra of CVO and SCVO are shown alongside the O and V PDOS from the LDA calculation. The low-energy shoulder at ~ 523 eV is due to the bonding states, and is relatively more intense for SCVO. This enhanced V-O hybridization is predicted by the LDA, in which the bonding O PDOS is predicted to be stronger for SrVO_3 compared with CaVO_3 , and is also reflected by the stronger V 3d – O 2p feature in the RXES measurements of SCVO (Fig. 1b). The discrepancy in the relative intensities of the bonding and non-bonding features between experiment and theory is most likely due to matrix element effects, which are not considered here. At higher energies, a substantial shoulder near 529 eV is observed, and can be attributed to the weak mixing of the O wavefunctions in the V 3d manifold. Additionally, approximately 1.5 eV below, there is a second poorly-resolved feature, which is slightly more intense for CVO than SCVO, and which appears at a gap in the LDA DOS. Tentatively, we speculate that this may represent emission from the LHB. If so, these spectra indicate that there is substantial mixing of the O 2p states with the LHB, and the assignment of the incoherent feature may be more complex than the LHB in its conventional meaning. Such a scenario has recently been proposed via extended cluster model calculations.[20] Further measurements and calculations are needed to accurately establish the nature of this feature.

In summary, we have shown that RXES is a sensitive *bulk* probe of correlated electron behavior in $\text{Sr}_x\text{Ca}_{1-x}\text{VO}_3$. The application of this technique to other correlated materials, particularly in tandem with ARPES measurements, may shed new light on the differences between electron correlations at the surface and in the bulk in systems such as topological insulators[23] and high- T_c superconductors[3]. In $\text{Sr}_x\text{Ca}_{1-x}\text{VO}_3$, we find better agreement in the energetics of the spectral features between DMFT[5, 12] and our RXES measurements than

we do with PES. Comparison with a thin-film sample supports our interpretation.

Acknowledgements. The authors would like to thank T. Balasubramanian for valuable discussions regarding the experiment. The Boston University program is supported in part by the Department of Energy under Grant No. DE-FG02-98ER45680. Supported also in part by the Boston University/University of War-

wick collaboration fund. The Advanced Light Source, Berkeley, is supported by the US Department of Energy under Contract No. DEAC02-05CH11231. G.B. gratefully acknowledges financial support from EPSRC Grant EP/I007210/1. M.G., J.W.L. and S.A.W. gratefully acknowledge financial support from the Army Research Office through MURI grant No. W911-NF-09-1-0398.

-
- [1] G. Kotliar, S. Y. Savrasov, K. Haule, V. S. Oudovenko, O. Parcollet and C. A. Marianetti, *Rev. Mod. Phys.* **78** 865 (2006).
 - [2] S. D. Kevan (Ed.), *Angle Resolved Photoemission*, Elsevier, Amsterdam (1991); A. Damascelli, *Phys. Scr.* **2004**, 61 (2004); T. Valla, A. V. Fedorov, P. D. Johnson and S. L. Hulbert, *Phys. Rev. Lett.* **83**, 2085 (1999); A. Hofmann, X. Y. Cui, J. Schäfer, S. Meyer, P. Höpfner, C. Blumenstein, M. Paul, L. Patthey, E. Rotenberg, J. Bünenmann, F. Gebhard, T. Ohm, W. Weber and R. Claessen, *Phys. Rev. Lett.* **102**, 187204 (2009); R. Eguchi, A. Chainani, M. Taguchi, M. Matsunami, Y. Ishida, K. Horiba, Y. Senba, H. Ohashi and S. Shin, *Phys. Rev. B* **79** 115122 (2009); X. Zhou, G. Liu, J. Meng, W. Zhang, H. Liu, L. Zhao and X. Jia, *Phys. Status Solidi A* **207**, 2674 (2010).
 - [3] J. D. Koralek, J. F. Douglas, N. C. Plumb, Z. Sun, A. V. Fedorov, M. M. Murnane, H. C. Kapteyn, S. T. Cundiff, Y. Aiura, K. Oka, H. Eisaki and D. S. Dessau *Phys. Rev. Lett.* **96**, 017005 (2006).
 - [4] K. E. Smith, C. McGuinness, J. E. Downes, P. J. Ryan, D. Fu, S. L. Hulbert, J. M. Honig and R. G. Egddell, *Mater. Res. Soc. Symp. Proc.* **755**, DD1.1.1 (2003).
 - [5] I. A. Nekrasov, G. Keller, D. E. Kondakov, A. V. Kozhevnikov, Th. Pruschke, K. Held, D. Vollhardt and V. I. Anisimov, *Phys. Rev. B* **72**, 155106 (2005).
 - [6] A. Sekiyama, H. Fujiwara, S. Imada, S. Suga, H. Eisaki, S. I. Uchida, K. Takegahara, H. Harima, Y. Saitoh, I. A. Nekrasov, G. Keller, D. E. Kondakov, A. V. Kozhevnikov, Th. Pruschke, K. Held, D. Vollhardt and V. I. Anisimov, *Phys. Rev. Lett.* **93** 156402 (2004).
 - [7] R. Eguchi, T. Kiss, S. Tsuda, T. Shimojima, T. Mizokami, T. Yokoya, A. Chainani, S. Shin, I. H. Inoue, T. Togashi, S. Watanabe, C. Q. Zhang, C. T. Chen, M. Arita, K. Shimada, H. Namatame and M. Taniguchi, *Phys. Rev. Lett.* **96** 076402 (2006).
 - [8] T. Yoshida, K. Tanaka, H. Yagi, A. Ino, H. Eisaki, A. Fujimori and Z.-X. Shen, *Phys. Rev. Lett.* **95**, 146404 (2005); M. Takizawa, M. Minohara, H. Kumigashira, D. Toyota, M. Oshima, H. Wadati, T. Yoshida, A. Fujimori, M. Lippmaa, M. Kawasaki, H. Koinuma, G. Sordi and M. Rozenberg, *Phys. Rev. B* **80**, 235104 (2009).
 - [9] T. Yoshida, M. Hashimoto, T. Takizawa, A. Fujimori, M. Kubota, K. Ono and H. Eisaki, *Phys. Rev. B* **82** 085119 (2010).
 - [10] S. Aizaki, T. Yoshida, K. Yoshimatsu, M. Takizawa, M. Minohara, S. Ideta, A. Fujimori, K. Gupta, P. Mahadevan, K. Horiba, H. Kumigashira and M. Oshima, *Phys. Rev. Lett.* **109** 056401 (2012).
 - [11] I. A. Nekrasov, K. Held, G. Keller, D. E. Kondakov, Th. Pruschke, M. Kollar, O. K. Andersen, V. I. Anisimov and D. Vollhardt, *Phys. Rev. B* **73** 155112 (2006); K. Byczuk, M. Kollar, K. Held, Y.-F. Yang, I. A. Nekrasov, Th. Pruschke and D. Vollhardt, *Nature Phys.* **3**, 168 (2007).
 - [12] H. Ishida, D. Wortmann and A. Liebsch, *Phys. Rev. B* **73** 245421 (2006).
 - [13] A. Liebsch, *Phys. Rev. Lett.* **90**, 096401 (2003).
 - [14] A. Kotani and S. Shin, *Rev. Mod. Phys.* **73**, 203 (2001); L. J. P. Ament, M. van Veenendaal, T. P. Devereaux, J. P. Hill and J. van den Brink, *Rev. Mod. Phys.* **83**, 705 (2011).
 - [15] I. H. Inoue, O. Goto, H. Makino, N. E. Hussey and M. Ishikawa, *Phys. Rev. B* **58**, 4372 (1998).
 - [16] M. Gu, J. Laverock, B. Chen, K. E. Smith, S. A. Wolf and J. Lu, *J. Appl. Phys.* **113**, 133704 (2013).
 - [17] H. Falcón, J. A. Alonso, M. T. Casais, M. J. Martínez-Lope and J. Sánchez-Benítez, *J. Solid State Chem.* **177**, 3099 (2004).
 - [18] J. K. Dewhurst, S. Sharma, L. Nordström, F. Cricchio, F. Bultmark and E. K. U. Gross, <http://elk.sourceforge.net> (2012).
 - [19] H. F. Pen, M. Abbate, A. Fujimori, Y. Tokura, H. Eisaki, S. Uchida and G. A. Sawatzky, *Phys. Rev. B* **59**, 7422 (1999).
 - [20] R. J. O. Mossaneck, M. Abbate, T. Yoshida, A. Fujimori, Y. Yoshida, N. Shirakawa, H. Eisaki, S. Kohno, P. T. Fonseca and F. C. Vicentin, *J. Phys.: Condens. Matter* **22**, 095601 (2010).
 - [21] J. Laverock, L. F. J. Piper, A. R. H. Preston, B. Chen, J. McNulty, K. E. Smith, S. Kittiwatanakul, J. W. Lu, S. A. Wolf, P.-A. Glans and J.-H. Guo, *Phys. Rev. B* **85**, 081104(R) (2012).
 - [22] Y. Aiura, H. Kawanaka, H. Bando and T. Yasue, *J. Vac. Sci. Technol. A* **19**, 1929 (2001).
 - [23] M. J. Schmidt, *Phys. Rev. B* **86**, 161110(R) (2012).